The Astrophysical Journal, 720:454–464, 2010 September 1 doi:10.1088/0004-637X/720/1/454


# SIGNATURES OF MAGNETIC RECONNECTION AT BOUNDARIES OF INTERPLANETARY SMALL-SCALE MAGNETIC FLUX ROPES

Hui Tian[1], Shuo Yao[1], Qiugang Zong[1], Jiansen He[2], and Yu Qi[1]
[1] School of Earth and Space Sciences, Peking University, 100871 Beijing, China; tianhui924@pku.edu.cn
[2] Max-Planck-Institut für Sonnensystemforschung, 37191 Katlenburg-Lindau, Germany
*Received 2010 March 24; accepted 2010 July 7; published 2010 August 11*

## ABSTRACT

The interaction between interplanetary small-scale magnetic flux ropes and the magnetic field in the ambient solar wind is an important topic in the understanding of the evolution of magnetic structures in the heliosphere. Through a survey of 125 previously reported small flux ropes from 1995 to 2005, we find that 44 of them reveal clear signatures of Alfvénic fluctuations and thus classify them as Alfvén wave trains rather than flux ropes. Signatures of magnetic reconnection, generally including a plasma jet of ∼30 km $s^{-1}$ within a magnetic field rotational region, are clearly present at boundaries of about 42% of the flux ropes and 14% of the wave trains. The reconnection exhausts are often observed to show a local increase in the proton temperature, density, and plasma beta. About 66% of the reconnection events at flux rope boundaries are associated with a magnetic field shear angle larger than 90° and 73% of them reveal a decrease of 20% or more in the magnetic field magnitude, suggesting a dominance of anti-parallel reconnection at flux rope boundaries. The occurrence rate of magnetic reconnection at flux rope boundaries through the years 1995–2005 is also investigated and we find that it is relatively low around the solar maximum and much higher when approaching solar minima. The average magnetic field depression and shear angle for reconnection events at flux rope boundaries also reveal a similar trend from 1995 to 2005. Our results demonstrate for the first time that boundaries of a substantial fraction of small-scale flux ropes have properties similar to those of magnetic clouds, in the sense that both of them exhibit signatures of magnetic reconnection. The observed reconnection signatures could be related either to the formation of small flux ropes or to the interaction between flux ropes and the interplanetary magnetic fields.

*Key words:* magnetic fields – plasmas – solar–terrestrial relations – solar wind

*Online-only material:* color figures

## 1. INTRODUCTION

Magnetic flux ropes, which are usually associated with eruptive processes in space and astrophysical plasmas, are helical magnetic field structures (e.g., Shitaba & Uchida 1986; Zong et al. 2004; Démoulin & Dasso 2009; Linton & Moldwin 2009; Cheng et al. 2010). Interplanetary magnetic flux ropes can be classified into two categories, the large-scale (∼day) magnetic clouds and small-scale (∼ hour) flux ropes (Cartwright & Moldwin 2008). Magnetic clouds, which are characterized by their high magnetic field magnitude, low proton temperature, and smooth rotation of the magnetic field direction through a large angle on the timescale of one day (e.g., Burlaga et al. 1981; Schwenn & Marsch 1991; Lepping et al. 2006; Jian et al. 2006), are believed to be a subset of interplanetary coronal mass ejections (ICMEs). The small-scale flux ropes, which exhibit a magnetic field behavior similar to their larger-scale counterparts, were discovered by Moldwin et al. (1995, 2000) through observations with the *Ulysses*, *IMP* 8, and *Wind* spacecraft. Unlike magnetic clouds, the proton density is often not depressed inside these small flux ropes. The small flux ropes are more likely to be observed in the slow rather than fast solar wind (Cartwright & Moldwin 2008; Feng et al. 2008). The small flux ropes are suggested to be the interplanetary manifestations of small-scale solar eruptions (Tu et al. 1997; Mandrini et al. 2005; Feng et al. 2007, 2008; Wu et al. 2008) or the products of local magnetic reconnection in the solar wind (Moldwin et al. 2000; Cartwright & Moldwin 2008; Ruan et al. 2009).

Magnetic reconnection is an important mechanism of energy conversion in space and astrophysical plasmas (e.g., Shitaba et al. 1994; Priest & Forbes 2000; Deng et al. 2004; Xiao et al. 2006; He et al. 2008, 2010). Although it has been suggested or predicted by many authors that such a process should be prevalent in the solar wind since tens of years ago, the observational signatures of magnetic reconnection have not been identified and recognized until recently. Gosling et al. (2005b) identified Petschek-type reconnection exhausts which are characterized by a roughly Alfvénic accelerated plasma jet confined to a region with rotational magnetic field and bounded by correlated changes in components of the magnetic field **B** and flow velocity **V** on one side and anti-correlated changes on the other. In the reconnection exhaust, the magnetic field magnitude is depressed, and as additional signatures, the proton density, temperature, and plasma beta are often locally enhanced. Subsequent intensive studies suggest that reconnection in the solar wind is often associated with extended X-lines (Phan et al. 2006; Gosling et al. 2007b) and are predominantly observed in the low-speed rather than high-speed solar wind (Gosling et al. 2006a; Gosling 2007; Phan et al. 2009). Only a few cases of reconnection have been found to be associated with the heliospheric current sheet (Gosling et al. 2005c, 2006b, 2007c). Local reconnection in the solar wind is not found to be efficient enough to produce energetic particles (Gosling et al. 2005a). Reconnection is found to be prevalent at small shear angles of the magnetic field (Gosling et al. 2007a; Gosling & Szabo 2008) in the low-beta solar wind (Phan et al. 2009).

Numerical simulations have shown that reconnection between coronal mass ejection (CME) flux ropes and the ambient magnetic field may play an important role in the evolution

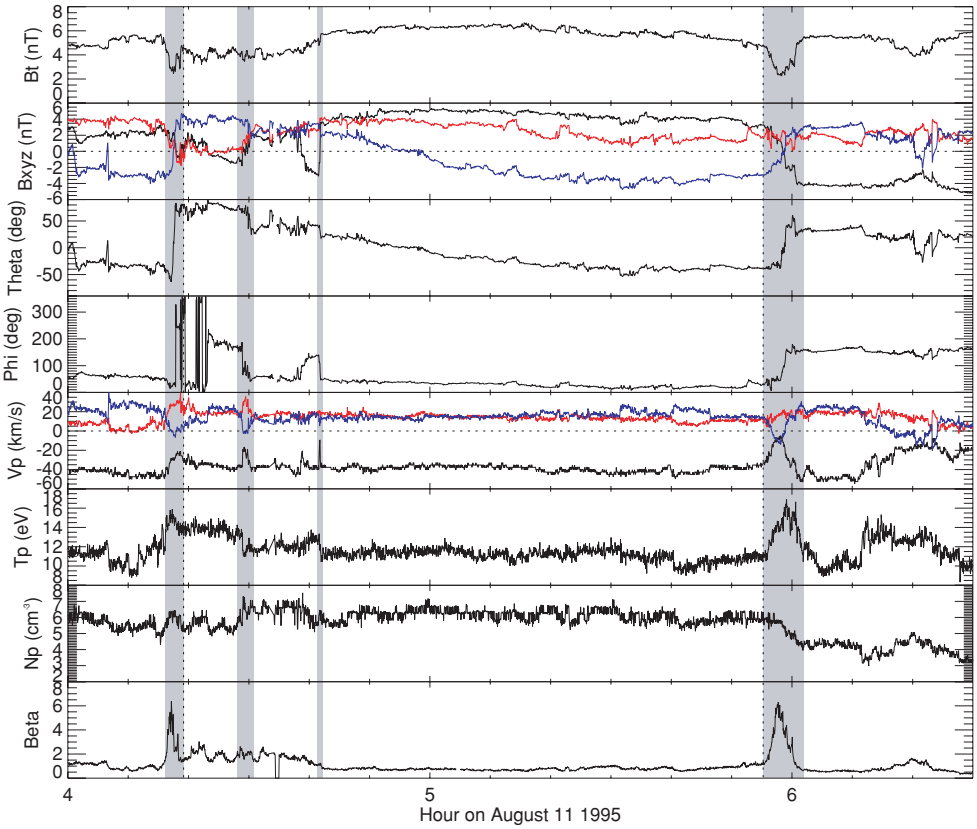


**Figure 1.** Magnetic field and plasma parameters for an interplanetary small-scale magnetic flux rope observed by *Wind* on 1995 August 11. From top to bottom: magnetic field magnitude (*Bt*), magnetic field vector in GSE Cartesian coordinates (*Bxyz*), elevation angle of the magnetic field (Theta), azimuthal angle of the magnetic field (Phi), proton velocity vector in GSE Cartesian coordinates (*Vxyz*), proton temperature (*Tp*), proton number density (*Np*), and plasma beta (Beta). The *x*-, *y*-, and *z*-components of the magnetic field and proton velocity are denoted by the black, red, and blue lines, respectively. A value of 450 km s$^{-1}$ has been added to the *x*-component of the velocity. The two dotted vertical lines mark the beginning and end of the flux rope. The shaded regions correspond to *Wind* crossing of reconnection exhausts.

(A color version of this figure is available in the online journal.)

of CMEs (e.g., Shiota et al. 2010). McComas et al. (1994) suggested that magnetic reconnection should commonly occur at the interfaces between fast ICMEs and the ambient solar wind. Some reported reconnection exhausts were indeed associated with ICMEs (e.g., Gosling et al. 2005b). Wei et al. (2003) found that most magnetic clouds have boundary layers displaying a drop in the magnetic field magnitude and a significant change in the field direction, as well as properties of a high proton temperature, density, and plasma beta. They claimed that these signatures are manifestations of magnetic reconnection through interaction between magnetic clouds and the ambient medium.

The interaction between interplanetary small-scale magnetic flux ropes and the magnetic field in the ambient solar wind is also an important topic but remains poorly understood. Feng & Wu (2009) reported a small flux rope followed by a reconnection exhaust. However, until now no systematic study of the boundaries of small flux ropes has been done. In this paper, we perform the first statistical investigation of the boundaries of interplanetary small-scale flux ropes and identify signatures of magnetic reconnection between the flux ropes and the interplanetary magnetic field.

## 2. CASE STUDIES AND DISCUSSION

Feng et al. (2008) performed a visual survey of the 1 minute averaged magnetic field and plasma data obtained by the *Wind* satellite and identified 125 small interplanetary magnetic flux ropes from 1995 to 2005 with the help of the Lundquist fitting technique (Lundquist 1950; Goldstein 1983). We started with this list of small flux ropes and investigated the properties of the rope boundaries by using the 3 s magnetic field and plasma data obtained by the Magnetic Field Investigation (MFI; Lepping et al. 1995) and 3DP (Lin et al. 1995) instrument on board *Wind*. A reconnection event (exhaust) was identified using the following primary criteria: (1) an obvious plasma jet within a region with rotational magnetic field and (2) at least one component of both the velocity change and the magnetic field change is correlated on one side and anti-correlated on the other side. As an interesting result, we found that clear signatures of magnetic reconnection are present at one or both boundaries of about 42% of the small flux ropes. Below, we show several examples before presenting the statistical results.

### *2.1. Magnetic Reconnection at Both Boundaries of the Flux Rope*

Figure 1 shows the magnetic field and plasma parameters for a typical small-scale flux rope observed on 1995 August 11. The two dotted vertical lines mark the beginning and end of the flux rope. Primary signatures of reconnection exhausts, plasma jets within the magnetic field rotational region, were clearly present at both boundaries of this flux rope.

The exhaust at the trailing boundary was observed from about 05:55 to 06:02. A strong decrease in the magnetic field magnitude (57%) was observed inside the exhaust. The plasma jets and magnetic field rotation mainly occurred in the *x*- and

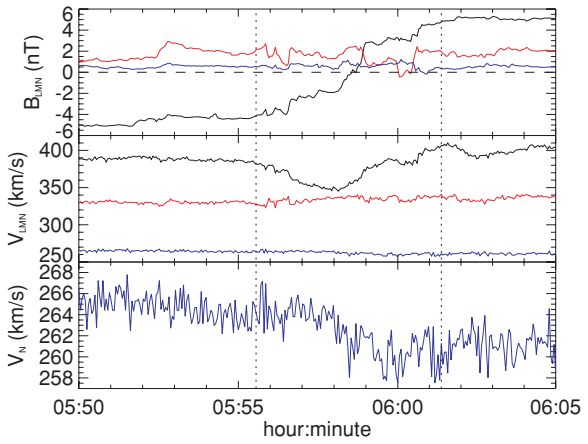


**Figure 2.** Reconnection exhaust observed by *Wind* around 06:00 on 1995 August 11. From top to bottom: magnetic field vector ($B_{LMN}$), velocity vector ($V_{LMN}$), and the *N*-component of the velocity ($V_N$). The *L*-, *M*-, and *N*-components of the magnetic field and proton velocity are denoted by the black, red, and blue solid lines, respectively. The two dotted vertical lines mark the beginning and end of the reconnection exhaust. A value of 200 km $s^{-1}$ has been added to the *M*-component of the velocity.

(A color version of this figure is available in the online journal.)

*z*-directions in the GSE coordinate system. In these two directions, we can see a clear anti-correlation between the changes of **B** and **V** at the front side and a correlation at the tail side of the exhaust. The shear angle of the magnetic field across the exhaust was relatively large (133°). Additional signatures of magnetic reconnection, including a local enhancement of the proton temperature and plasma beta, were also observed in the exhaust. The proton density was not enhanced but intermediate to those on the opposite sides of the exhaust, indicating that the transitions from the ambient medium to the exhaust are not slow-mode-like on both sides (Gosling et al. 2006a).

We performed a minimum variance analysis (MVA) of the magnetic field from 05:50 to 06:05 and established the *LMN* coordinate system for the reconnecting current sheet (Sonnerup & Cahill 1967; Davis et al. 2006; Phan et al. 2006). The magnetic field rotated predominantly in the *L*-direction, which was [−0.78, 0.01, 0.63] in GSE Cartesian coordinates. The *M*-direction aligning with the X-line orientation was found to be [−0.26, 0.91, −0.32] in GSE. The overall current sheet normal, the *N*-direction, was [0.57, 0.41, 0.71] in GSE. Figure 2 shows the magnetic fields and proton velocities as converted to the *LMN* coordinates. In the direction normal to the current sheet, the proton velocity across the exhaust is differentiated by about 4 km $s^{-1}$, indicating an inflow velocity of 2 km $s^{-1}$ in the frame of the current sheet. The reconnection electric field was estimated to be 0.01 mV $m^{-1}$, with a magnetic field of about 5 nT convecting into the reconnection region at this inflow speed. The dimensionless reconnection rate, the inflow speed divided by the Alfvén speed, was calculated to be about 5%, indicating fast reconnection (Davis et al. 2006; Phan et al. 2006).

In the list of Feng et al. (2008), the duration of this flux rope was from 04:41 to 05:56. From Figure 1, we can clearly see a reconnection exhaust just at about 04:41. This exhaust only lasted for about 18 s, and the magnetic field reversal and plasma jet were mainly present in the *x*-direction. However, if we look at the overall behavior of the magnetic field elevation angle of this flux rope, we can see an almost smooth variation starting at 04:19. From about 04:16 to 04:19, an abrupt large rotation of the elevation angle accompanied by all typical signatures of magnetic reconnection was observed. A strong depression of the magnetic field magnitude (44%) and a large shear angle (143°) of the magnetic field vectors were associated with this reconnection exhaust. We think that it is more appropriate to use this reconnection event as the leading boundary of the flux rope. In fact, the leading boundary of this flux rope seems to be a complex layer rather than a simple edge. This layer may correspond to the time interval from 04:16 to 04:41. Between the reconnection exhaust around 04:19 and the one around 04:41, we even found a third possible reconnection exhaust at about 04:29 within the leading boundary layer. These findings suggest that the interaction between small-scale flux ropes and the ambient solar wind can be very complicated.

Another example of magnetic reconnection at both boundaries of a flux rope is presented in Figure 3. This flux rope was encountered by *Wind* on 2004 March 5. According to Feng et al. (2008), the duration of this flux rope was from 02:41 to 04:12. A reconnection exhaust occurring at about 02:41 was present just ahead of the flux rope, while another one starting at about 04:13 was observed just behind the flux rope. At the leading boundary, the jet was found in the *x*- and *z*-directions in the GSE coordinate system, while at the trailing boundary the jet was mainly found in the *z*-direction. A relatively weak (26%) depression of the magnetic field magnitude was present in the leading boundary, while at the trailing boundary a very strong (75%) decrease was observed. The magnetic field shear angles across the two exhausts were found to be 92° and 161°, respectively. Both exhausts revealed a local enhancement in the proton temperature, density, and plasma beta, consistent with Petschek's theory that the reconnection exhausts are bounded by a slow-mode wave on both sides (Petschek 1964).

### *2.2. Magnetic Reconnection at one Boundary of the Flux Rope*

Signatures of magnetic reconnection were not always present on both boundaries of small-scale flux ropes. In many cases, reconnection exhausts were only observed to be associated with the leading or trailing boundaries of flux ropes.

Feng & Wu (2009) reported a small flux rope followed by a reconnection exhaust and suggested that the magnetic fields of the flux rope were peeled off through the reconnection between the flux rope and the background solar wind. However, it seems that this event was inside the leading boundary layer of a near-Earth ICME starting at about 13:00 on 1998 March 25 and ending at 10:00 on 1998 March 26 (Cane & Richardson 2003). This small flux rope might correspond to the second flux rope produced along with the CME flux rope as predicted by the breakout model of van der Holst et al. (2007). And the reconnection might be the result of the interaction between the small flux rope and the ICME.

A reconnection exhaust at the leading boundary of a flux rope observed by *Wind* on 2005 March 5 is shown in Figure 4. The reconnection exhaust was encountered by *Wind* within 80 s, beginning at 07:26:35. A rotation of the magnetic field direction can be identified mainly from the *y*-component. Correspondingly, an obvious jetting plasma was present in the *y*-direction. The changes of the magnetic field and proton velocity were correlated on the front side and anti-correlated on the tail side of the exhaust. Obvious enhancements of the proton density, temperature, and plasma beta were all observed inside the exhaust. The magnetic field magnitude decreased 33% in the exhaust. After crossing the exhaust, the magnetic field direction changed by 135°. No reconnection exhaust was observed at the trailing boundary of this flux rope.

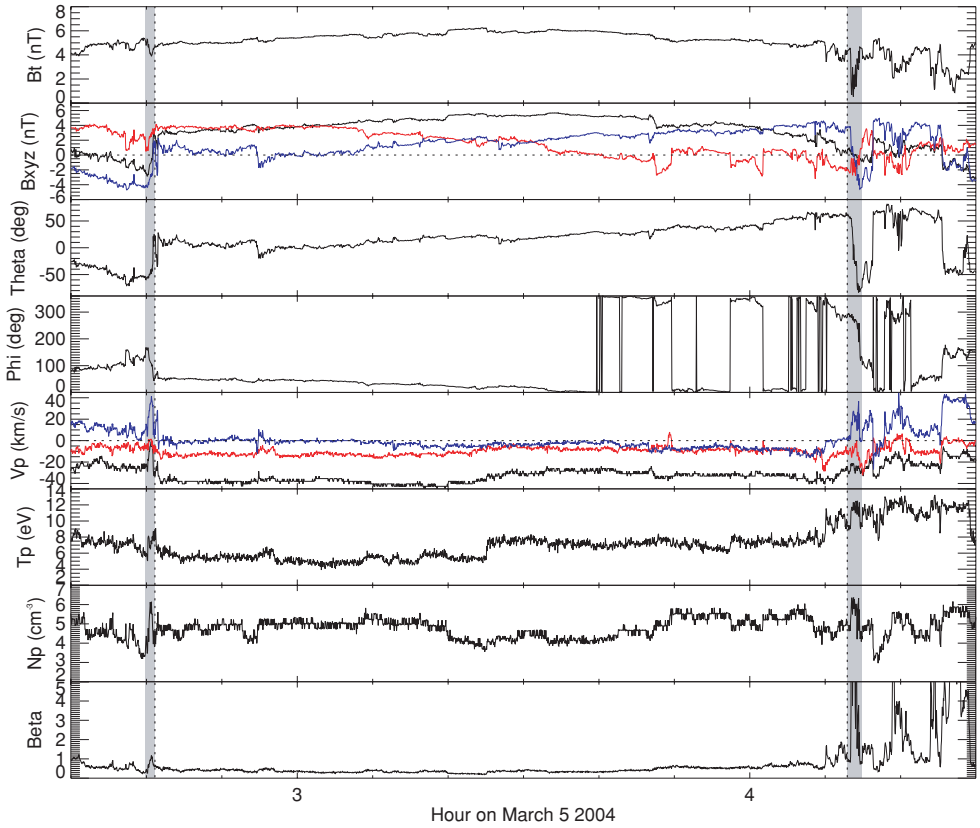


**Figure 3.** Magnetic field and plasma parameters for an interplanetary small-scale magnetic flux rope observed by *Wind* on 2004 March 5. A value of 450 km s$^{-1}$ has been added to the *x*-component of the velocity.

(A color version of this figure is available in the online journal.)

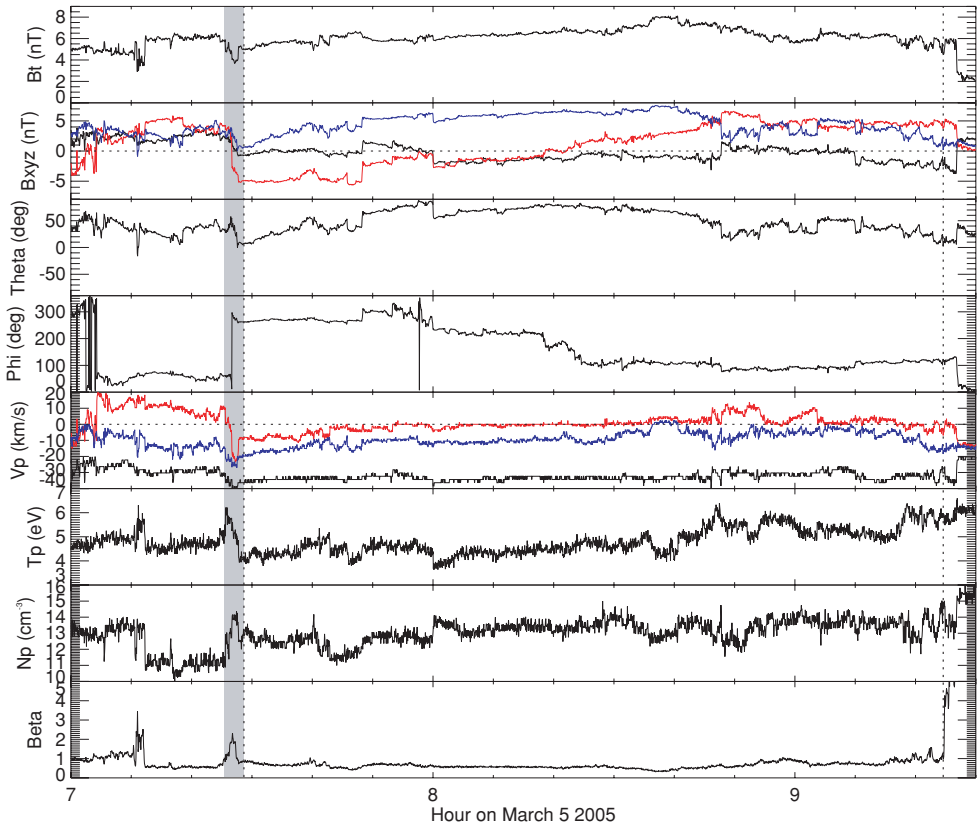


**Figure 4.** Magnetic field and plasma parameters for an interplanetary small-scale magnetic flux rope observed by *Wind* on 2005 March 5. A value of 380 km s$^{-1}$ has been added to the *x*-component of the velocity.

(A color version of this figure is available in the online journal.)

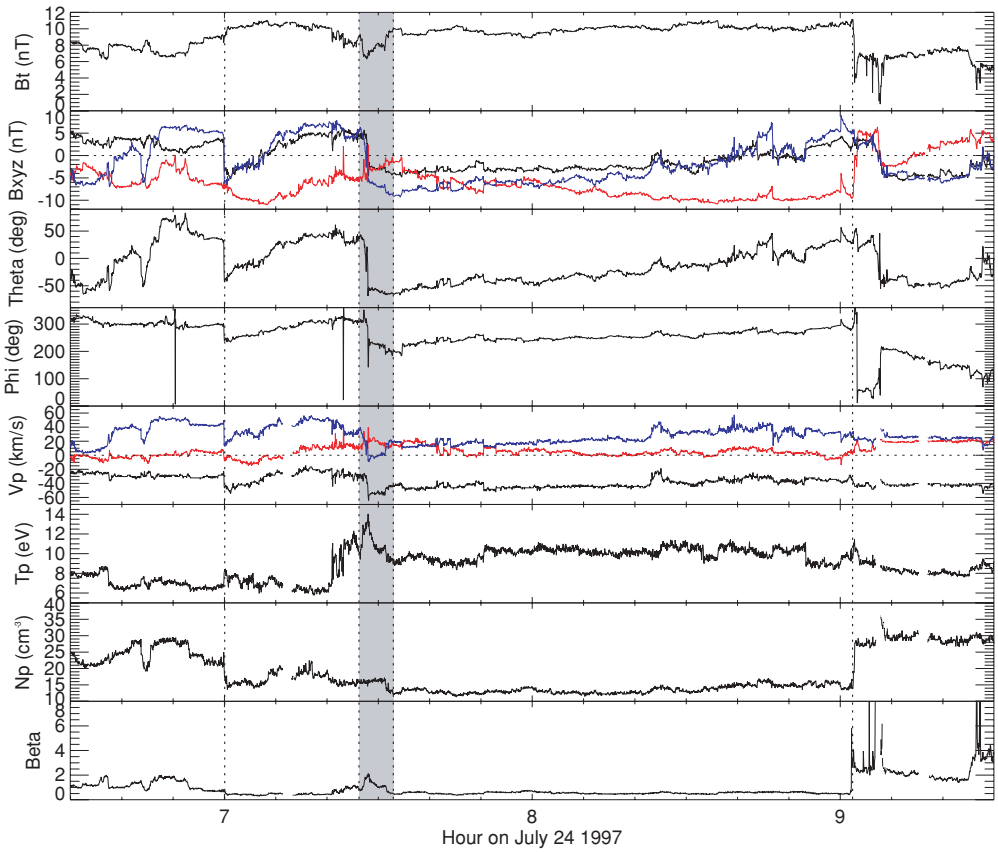


**Figure 5.** Magnetic field and plasma parameters for two interplanetary small-scale magnetic flux ropes observed by *Wind* on 1997 July 24. A value of 370 km s$^{-1}$ has been added to the *x*-component of the velocity. A reconnection exhaust was observed between the two flux ropes.

(A color version of this figure is available in the online journal.)

In the list of Feng et al. (2008), there are two flux ropes which were observed by *Wind* one after the other on 1997 July 24. Figure 5 shows the magnetic field and plasma parameters of these two cases. The first flux rope encountered by *Wind* was from about 07:00 to 07:26 and the second one was from 07:32 to 9:02. Interestingly, we clearly found a reconnection exhaust between these two flux ropes. The plasma jet was primarily observed in the *x*- and *z*-components. The magnetic field decreased by about 22% inside the exhaust, and a shear angle of 132° was observed across the exhaust. The exhaust was immediately preceded by the first rope and immediately followed by the second one. The bipolar signatures of the two flux ropes were both present in the *x*- and *z*-directions, indicating a similar orientation of the two flux ropes. Indeed, the longitude and latitude angles of the two ropes' axes in the ecliptic coordinate system, which were [209°,−12°] and [281°,−6°], as obtained from the fitting with the Lundquist solution in Feng et al. (2008), were not so different. Imagining two adjacent flux ropes with the same handedness aligned in a similar orientation, we can find that an almost anti-parallel magnetic field configuration will form between the two ropes. This configuration is favorable for the occurrence of magnetic reconnection. So, the reconnection event we observed seems to be the result of interactions between the two small-scale flux ropes.

## 3. STATISTICAL RESULTS AND DISCUSSION

We surveyed the entire list of 125 flux ropes in Feng et al. (2008) and identified 47 reconnection exhausts at one or two boundaries of these possible flux ropes. The starting and ending time of the reconnection events and their associated flux ropes are listed in Table 1. The decrease of the magnetic field magnitude inside the reconnection exhausts (%) and the shear angles of magnetic field across the reconnection exhausts (°) are also shown there.

### *3.1. Detection of Alfvénic Fluctuations*

Cartwright & Moldwin (2008) mentioned that some Alfvén wave trains might show observational magnetic field properties similar to flux ropes. An inspection of the magnetic field and velocity data of flux ropes listed in Feng et al. (2008) suggested that some of these flux ropes revealed clear signatures of Alfvén waves. We designed an automatic algorithm to recognize these wave trains. We first smoothed the magnetic field **B** and proton velocity **V** over 20 minutes, respectively. Fluctuations of the magnetic field and velocity were then obtained by subtracting the smoothed data from the original data. The resulting magnetic field perturbations were used to calculate the Alfvén velocity fluctuations using the formula $\delta \mathbf{V}_b = \delta \mathbf{B}/\sqrt{\mu\rho}$. Here, $\delta \mathbf{B}$, $\mu$, and $\rho$ refer to the magnetic field perturbation, permeability of free space, and proton mass density, respectively. Finally, the correlation coefficients between the components of the Alfvén velocity and proton velocity perturbations were calculated. Flux ropes listed in Feng et al. (2008) were determined to be Alfvén wave trains if two or three of the correlation coefficients are larger than 0.6. This method is similar to Denskat & Burlaga (1977) except for the inclusion of the density effect here. Alfvén wave trains and the rest flux ropes are marked in Table 1 as "A" and "F," respectively.

**Table 1**
Reconnection Exhausts at Boundaries of Interplanetary Small-scale Magnetic Flux Ropes

| Number | Year | $T_{fb}$[a] | $T_{fe}$[b] | L[c] | $T_{rb}$[d] | $T_{re}$[e] | D[f] | S[g] | A[h] |
|---|---|---|---|---|---|---|---|---|---|
| 1 | 1995 | 03072317 | 03080043 | T | 004330 | 004830 | 46 | 56 | A |
| 2 | 1995 | 03241125 | 03241615 | L | 112000 | 112430 | 7 | 40 | F |
| 3 | 1995 | 05131025 | 05131625 | L | 102330 | 102435 | 45 | 54 | F |
| 4 | 1995 | 06172140 | 06180441 | L | 213850 | 214010 | 31 | 155 | F |
| 5 | 1995 | 06172140 | 06180441 | T | 044025 | 044105 | 16 | 62 | F |
| 6 | 1995 | 08110419 | 08110555 | L | 041555 | 041900 | 44 | 143 | F |
| 7 | 1995 | 08110419 | 08110555 | T | 055500 | 060200 | 57 | 133 | F |
| 8 | 1995 | 08151419 | 08151800 | L | 141200 | 141900 | 50 | 115 | F |
| 9 | 1995 | 08151419 | 08151800 | T | 180025 | 180245 | 29 | 139 | F |
| 10 | 1995 | 09201301 | 09201401 | L | 125730 | 130030 | 70 | 156 | F |
| 11 | 1995 | 09210254 | 09210454 | L | 025240 | 025320 | 40 | 111 | F |
| 12 | 1996 | 02101741 | 02102207 | T | 220730 | 220845 | 4 | 56 | F |
| 13 | 1996 | 03081947 | 03090235 | T | 023545 | 023645 | 11 | 104 | F |
| 14 | 1996 | 03130927 | 03131021 | L | 092540 | 092630 | 86 | 169 | F |
| 15 | 1996 | 05020541 | 05020647 | L | 054010 | 054030 | 50 | 159 | F |
| 16 | 1996 | 05170101 | 05170955 | T | 095500 | 095545 | 27 | 79 | F |
| 17 | 1996 | 09281234 | 09281440 | L | 123145 | 123400 | 42 | 121 | F |
| 18 | 1996 | 09281234 | 09281440 | T | 144025 | 144125 | 71 | 168 | F |
| 19 | 1997 | 05111141 | 05111401 | T | 140145 | 140310 | 19 | 123 | F |
| 20 | 1997 | 05120524 | 05120741 | T | 074115 | 074230 | 20 | 51 | F |
| 21 | 1997 | 05230616 | 05231218 | L | 061400 | 061550 | 54 | 68 | F |
| 22 | 1997 | 05240222 | 05240740 | T | 073955 | 074010 | 21 | 71 | F |
| 23 | 1997 | 05251910 | 05260244 | L | 190900 | 190950 | 29 | 98 | A |
| 24 | 1997 | 07240700 | 07240726 | T | 072630 | 073230 | 22 | 132 | F |
| 25 | 1997 | 07240732 | 07240902 | L | 072630 | 073230 | 22 | 132 | F |
| 26 | 1998 | 03251328 | 03251616 | T | 161600 | 162300 | 41 | 154 | F |
| 27 | 1998 | 06021030 | 06021635 | T | 163505 | 163610 | 22 | 95 | A |
| 28 | 1998 | 06260004 | 06260750 | T | 075000 | 075015 | 13 | 91 | F |
| 29 | 2000 | 04181524 | 04181743 | L | 152325 | 152345 | 7 | 43 | A |
| 30 | 2000 | 04210635 | 04210932 | L | 063300 | 063500 | 13 | 84 | A |
| 31 | 2000 | 08230923 | 08231158 | T | 115850 | 115915 | 9 | 14 | F |
| 32 | 2000 | 12231554 | 12232137 | L | 155420 | 155520 | 9 | 85 | F |
| 33 | 2001 | 01090242 | 01090325 | T | 032500 | 032550 | 13 | 147 | F |
| 34 | 2001 | 09261026 | 09261717 | L | 102500 | 102530 | 4 | 18 | F |
| 35 | 2001 | 09261026 | 09261717 | T | 171700 | 171730 | 14 | 89 | F |
| 36 | 2002 | 01192108 | 01192145 | T | 214450 | 214630 | 32 | 142 | F |
| 37 | 2002 | 02182306 | 02190249 | L | 230135 | 230535 | 8 | 93 | F |
| 38 | 2002 | 03171932 | 03172116 | L | 193010 | 193130 | 8 | 66 | F |
| 39 | 2003 | 04291641 | 04291852 | L | 163930 | 164050 | 40 | 120 | F |
| 40 | 2003 | 04291641 | 04291852 | T | 185200 | 190700 | 40 | 93 | F |
| 41 | 2003 | 08050824 | 08051021 | L | 081700 | 082400 | 20 | 114 | A |
| 42 | 2003 | 09292209 | 09300134 | T | 013450 | 013650 | 22 | 71 | F |
| 43 | 2004 | 03050241 | 03050413 | L | 024005 | 024100 | 26 | 92 | F |
| 44 | 2004 | 03050241 | 03050413 | T | 041315 | 041450 | 75 | 161 | F |
| 45 | 2004 | 08022335 | 08030100 | L | 233300 | 233410 | 21 | 120 | F |
| 46 | 2005 | 03050728 | 03050924 | L | 072635 | 072755 | 33 | 135 | F |
| 47 | 2005 | 11110011 | 11110052 | T | 005230 | 010000 | 70 | 143 | F |

**Notes.**
[a] The beginning of the flux ropes, MonthDayHourMinute UT.
[b] The end of the flux ropes, MonthDayHourMinute UT.
[c] The leading (L) or trailing (T) boundaries of the flux ropes.
[d] The beginning of the reconnection exhausts, HourMinuteSecond UT.
[e] The end of the reconnection exhausts, HourMinuteSecond UT.
[f] The decrease of the magnetic field inside the reconnection exhausts (%).
[g] The shear angles of magnetic field across the reconnection exhausts (degree).
[h] Identified as flux ropes (F) or Alfvén wave trains (A).

Figure 6 shows the evolution of the components of the Alfvén velocity and proton velocity perturbations for an identified Alfvén wave train. The correlation coefficients for the three components are 0.62, 0.87, and 0.91, respectively. These high correlations, especially for the *y*- and *z*-components, indicate that Alfvén waves are clearly present.

According to Cartwright & Moldwin (2008), structures with clear Alfvénic fluctuations should be rejected as possible flux ropes. However, it might be possible that these Alfvén waves were generated inside the flux ropes. Okamoto et al. (2007) identified transverse oscillations of fine-scale threads in solar prominences and interpreted them as Alfvén waves. If these waves are

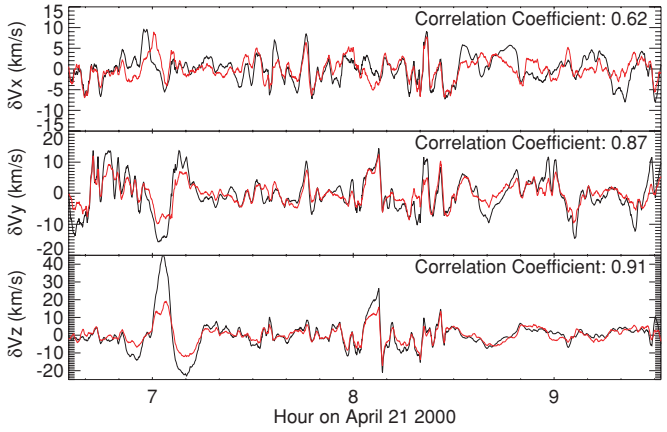


**Figure 6.** Evolution of the components of the Alfvén velocity (black) and proton velocity (red) perturbations for an Alfvén wave train observed by *Wind* on 2000 April 21. The correlation coefficients are also shown in each panel.

(A color version of this figure is available in the online journal.)

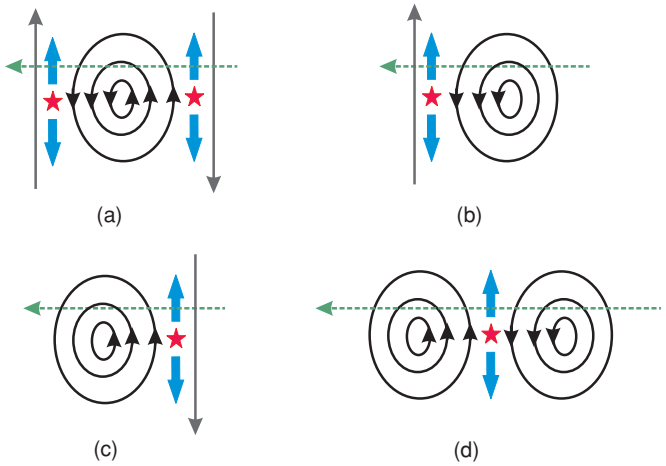


**Figure 7.** Panels (a)–(c): magnetic reconnection between interplanetary flux ropes (black) and the ambient magnetic field (gray). (d): magnetic reconnection between two adjacent flux ropes. The stars and blue arrows represent reconnecting X-points and outflows, respectively. The long dashed arrows indicate trajectories of *Wind*. The Sun is to the left.

(A color version of this figure is available in the online journal.)

carried by erupting prominences into the interplanetary space, they should be observed in situ as correlated changes between the magnetic field and velocity. In fact, signatures of Alfvén waves have already been found in magnetic clouds (Marsch et al. 2009; Yao et al. 2010). If small-scale magnetic flux ropes are interplanetary manifestations of small-scale solar eruptions (Feng et al. 2007, 2008), and Alfvén waves generated in small-scale solar activities (Mandrini et al. 2005; Innes et al. 2009) are carried outward through their eruptions to the interplanetary space, it will not be strange to observed the Alfvénic fluctuations in small-scale flux ropes. On the other hand, if small-scale flux ropes are the products of local magnetic reconnection in the solar wind (Moldwin et al. 2000; Cartwright & Moldwin 2008), Alfvén waves could also form since magnetic reconnection can generate the waves.

Although we do not exclude the possibility that some Alfvén wave trains might also be real magnetic flux ropes with intrinsic Alfvénic fluctuations, we decide to follow Cartwright & Moldwin (2008) and classify those Alfvén wave trains we identified under a different group rather than as flux ropes, since we cannot provide any evidence to prove that these waves are generated inside magnetic flux ropes.

### *3.2. Properties of Magnetic Reconnection at Flux Rope Boundaries*

Among the 125 small-scale flux ropes in Feng et al. (2008), we found 44 cases with clear Alfvénic fluctuations and classified them into Alfvén wave trains. The remaining 81 cases were classified as real magnetic flux ropes. We found that 42% (34/81) of the flux ropes have signatures of magnetic reconnection at one or two of their boundaries, while only 14% (6/44) of the wave trains reveal reconnection signatures at their boundaries. This result suggests that the probability of magnetic reconnection is very high at flux rope boundaries. The lower probability of reconnection associated with wave trains than that associated with flux ropes also indicates that the wave trains and flux ropes are likely to be different structures, thus supporting our classification mentioned above.

In the highly turbulent solar wind, the ambient interplanetary magnetic field (IMF) is often observed to change its direction away from the Parker spiral locally. The well-organized magnetic field lines of a flux rope can be expected to be obviously sheared with respect to the ambient IMF, resulting in the formation of a current sheet and sometimes reconnection on the leading, trailing, or both sides, as demonstrated in Figures 1–5 and sketched in Figures 7(a)–(c). On the other hand, as will be discussed in Section 3.4, the reconnection process might also be related to the formation of flux ropes in the heliospheric current sheet.

The distributions of the minimum reconnection duration, shear angle of the magnetic field across the reconnection exhaust, and percentage of the magnetic field depression for the reconnection events associated with flux ropes and wave trains are presented in Figure 8. The minimum reconnection duration, represented by the observed exhaust duration, peaks at the first bin for both the flux ropes and wave trains, indicating that in both cases most of the reconnecting boundary layers are very thin.

We found that about 66% of the reconnection events at flux rope boundaries are associated with a magnetic field shear angle larger than 90°. Figure 8 clearly reveals that large shear angles are predominant for reconnection at flux rope boundaries. The shear angle for reconnection associated with Alfvén wave trains ranges from 40° to 120°. The average shear angles for the two are 107° and 82°, respectively. Our result indicates that at boundaries of flux ropes the anti-parallel field component usually exceeds the guide field component, resulting in fast anti-parallel reconnection. Through a statistical study, Gosling et al. (2007a) concluded that magnetic reconnection in the solar wind occurs more frequently at shear angles smaller than 90° and is associated with relatively low reconnection rates. Thus, considering the shear angles, magnetic reconnection in the background solar wind is largely different from that at boundaries of small-scale magnetic flux ropes.

The depression of the magnetic field magnitude is larger than 20% for most reconnection exhausts associated with both flux ropes (73%) and wave trains (67%). We also investigated the field depression at flux rope boundaries without reconnection signatures and found that in most cases (64%), the field depression is less than 20%. Figure 9 shows the relationship between the magnetic field depressions inside reconnection exhausts and shear angles of the magnetic field across the

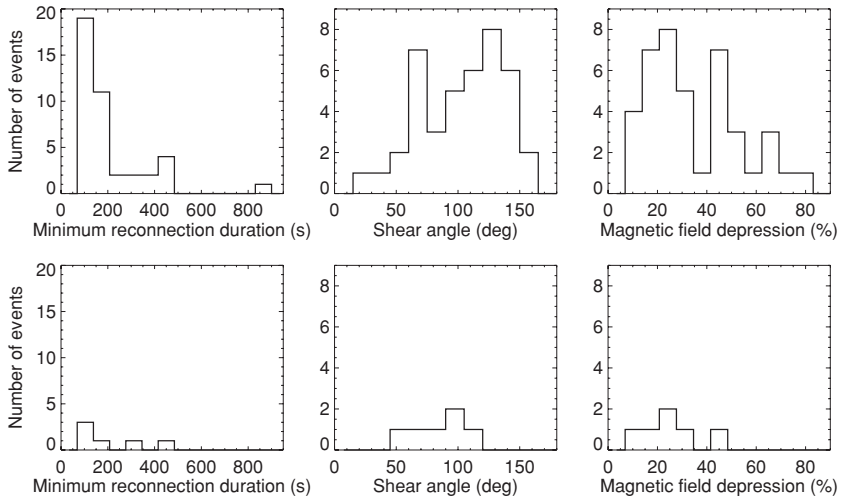


**Figure 8.** Distributions of the minimum reconnection duration (left), shear angle of the magnetic field across the reconnection exhaust (middle), and percentage of the magnetic field depression (right). Results for the flux ropes and Alfvén wave trains are presented in the top and bottom panels, respectively.

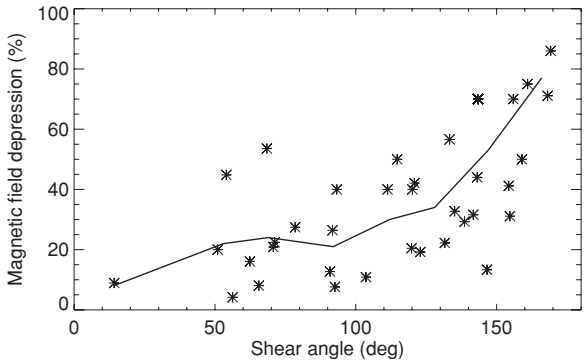


**Figure 9.** Relationship between the magnetic field depressions inside reconnection exhausts and shear angles of the magnetic field across the exhausts. Each asterisk represents one reconnection event at one boundary of a flux rope. The line shows the average field depressions in nine shear-angle bins.

exhausts. We divided the shear angle into nine bins and averaged the field depression in each bin (see the solid line in Figure 9). Although large scatters are present, we can still see a clear trend of enhancement in the magnetic field depression with increasing shear angle, indicating that very strong magnetic field depressions (e.g., larger than 35%) are often associated with large shear angles and thus anti-parallel reconnection.

We also investigated the occurrence rate of magnetic reconnection, average shear angle across reconnection exhausts, and average magnetic field depression inside reconnection regions at flux rope boundaries through the years 1995–2005. Figure 10 shows the result. We found that the probability of reconnection at small-scale flux rope boundaries is relatively low around the solar maximum and very high when approaching the solar minima. Note that no reconnection event was found at the boundaries of flux ropes in 1999. A low occurrence rate was found in 1999 for both magnetic clouds and small-scale flux ropes (Cartwright & Moldwin 2008; Feng et al. 2008). The low occurrence rate of magnetic clouds was suggested to be due to the fact that the CME sources migrated to higher latitudes of the Sun in 1999 (Gopalswamy et al. 2003), and the low occurrence rate of small-scale flux ropes might also be related to the solar activity (Feng et al. 2008). Our result further indicates that at the year of low occurrence of small-scale flux ropes, the occurrence rate of reconnection at flux rope boundaries is also depressed.

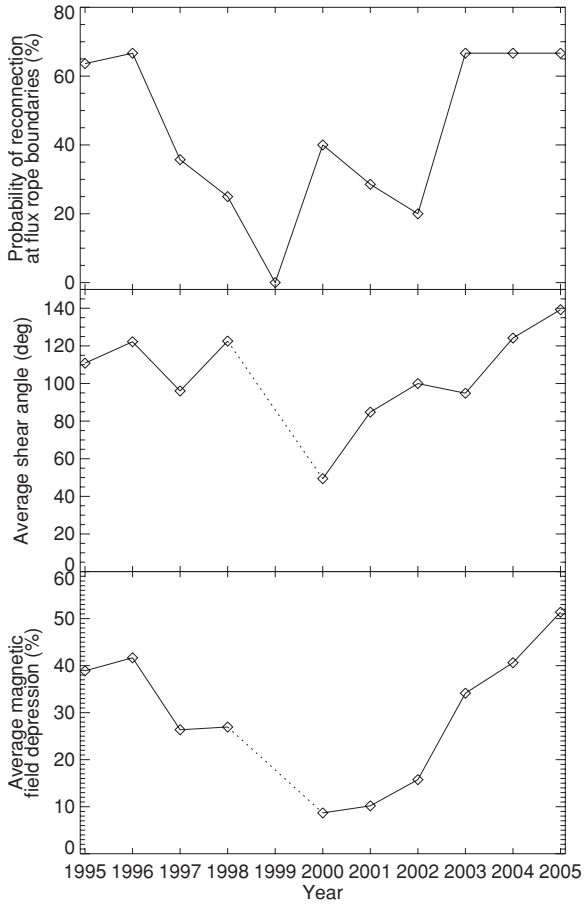


**Figure 10.** Probability of magnetic reconnection, average shear angle across reconnection exhausts, and average magnetic field depression inside reconnection regions at flux rope boundaries from 1995 to 2005.

Interestingly, the temporal variations of the average shear angle and magnetic field depression, particularly the latter, also reveal a similar trend. We speculate that at solar maximum the more complex magnetic field structures both on the Sun and in the solar wind might be responsible for these behaviors. More observational analyses are needed to confirm and explain these results.

### 3.3. Comparison between Small-scale Flux Ropes and Magnetic Clouds

So far we have demonstrated that signatures of magnetic reconnection are present at boundaries in 42% of the small-scale flux ropes. Wei et al. (2003) found that substantial parts of magnetic clouds have boundary layers displaying a drop in the magnetic field magnitude and a significant change of the field direction, as well as high proton temperature, density, and plasma beta. They claimed that these signatures are manifestations of magnetic reconnection through interactions between magnetic clouds and the ambient medium. The small-scale flux rope boundaries studied by us exhibit characteristics very similar to boundaries of large-scale magnetic clouds, implying a similar interaction process between these flux ropes and the magnetic field in the ambient medium. This similarity might also suggest that some of the interplanetary small-scale magnetic flux ropes have an origin similar to the magnetic clouds (Feng et al. 2007, 2008; Feng & Wu 2009).

However, Wei et al. (2003) did not check if the roughly Alfvénic plasma jets are prevalent at magnetic cloud boundaries. It would be interesting to investigate if the Petschek-type reconnection exhausts (e.g., Gosling et al. 2005b) are present in the boundary layers of magnetic clouds. Wei et al. (2003) mentioned that features of magnetic reconnection regions are observed more frequently at the leading boundaries of magnetic clouds than at the trailing boundaries. In Table 1, the number of reconnection events occurring at the leading and trailing boundaries of small-scale flux ropes are 20 and 21, respectively. So, it seems that the chance of reconnection is comparable at both boundaries of small flux ropes.

Furthermore, we noted that there are only seven small-scale flux ropes exhibiting signatures of reconnection at both boundaries, and more than half of the small-scale magnetic flux ropes do not exhibit signatures of magnetic reconnection at their boundaries. This result might be related to magnetic field configurations at the interfaces between flux ropes and the ambient medium, the restriction of the temporal resolution, and the non-persistence of the reconnection process. A small shear angle or a gentle variation of the magnetic field across the interfaces may not be favorable for the occurrence of magnetic reconnection. It is known that a higher time resolution of the instrument leads to the discovery of more reconnection events (Gosling & Szabo 2008; Phan et al. 2009); the 3 s resolution of the instruments might not be sufficient to resolve some very narrow reconnection exhausts present at flux rope boundaries. Wei et al. (2003) mentioned that reconnection conditions might be weakened as the magnetic reconnection at boundary layers of magnetic clouds proceeds, resulting in the recovery of the frozen-in condition. The process may continuously repeat and lead to intermittent magnetic reconnection. This scenario may also be the case at the boundaries of small-scale flux ropes and could be one of the reasons of the observed low occurrence rate of magnetic reconnection.

As mentioned in Section 2.2, Figure 5 shows an example of reconnection between two adjacent small-scale flux ropes. This scenario is sketched in Figure 7(d). As the reconnection proceeds, the two flux ropes could coalesce and thus grow in size, as demonstrated in laboratory experiments and numerical simulations (e.g., Furno 2005; Richard et al. 1989; Linton 2006). The two adjacent small flux ropes might also be the small-scale counterpart of multiple magnetic clouds (e.g., Wang et al. 2002, 2005; Xiong et al. 2007, 2009).

### 3.4. Origin of Interplanetary Small-scale Magnetic Flux Ropes

There is a debate regarding the origin of interplanetary small-scale magnetic flux ropes. Moldwin et al. (2000) and Cartwright & Moldwin (2008) suggested that these small flux ropes are produced through interplanetary magnetic reconnection, while others proposed that they are interplanetary manifestations of small-scale solar eruptions (Feng et al. 2007, 2008; Wu et al. 2008). Wei et al. (2003) and Pick et al. (2005) mentioned that the magnetic field lines of relatively large flux ropes originating from the Sun could be peeled off through magnetic reconnection away from the Sun. Feng & Wu (2009) reported a small flux rope followed by a reconnection exhaust and suggested that the small flux rope is produced through this peeling off process.

Compared to Feng & Wu (2009), our statistic result provides many more cases of small flux ropes with signatures of magnetic reconnection at their boundaries. Our result clearly reveals that magnetic reconnection is common at the interfaces between small flux ropes and the ambient medium. However, it is still an open question whether this reconnection is related to the formation of small flux ropes or not. In the scenario suggested by Feng & Wu (2009), the flux rope can be diminished in size due to reconnection with the ambient magnetic field as it moves from the Sun to the Earth. However, such shrinking has not been directly observed in interplanetary space. On the contrary, large-scale flux ropes such as magnetic clouds usually show a decrease in the measured plasma velocity as they pass the spacecraft, indicating an expansion in size when moving away from the Sun (e.g., Lepping et al. 2006). A recent study of Cartwright & Moldwin (2010) completed a comprehensive survey of interplanetary small flux ropes observed between 0.3 and 5.5 AU using the *Helios*, *IMP 8*, *Wind*, *ACE*, and *Ulysses* data and found that on average the size of small flux ropes expands rapidly within 1 AU and then reaches equilibrium in the outer heliosphere. These results seem to indicate that the expansion process dominates over the peeling off process for flux ropes originating from the Sun, which is inconsistent with the scenario that small flux ropes are produced through the peeling off of magnetic field lines in the outer layers of magnetic clouds.

In Earth magnetospheric studies, multiple X-line reconnections (Lee et al. 1985) are believed to be responsible for the observed flux rope chains in the plasma sheet of the magnetotail (e.g., Slavin et al. 2003; Zong et al. 2004; Eastwood et al. 2005; Liu et al. 2009). In principle, flux ropes could also be produced through a similar process in interplanetary space. Observations reveal that small-scale flux ropes lack a signature of expansion and are not depressed in proton temperature, which are distinctly different from magnetic clouds. Moreover, some small flux ropes were observed near the sector crossing (heliospheric current sheet crossing). These observational facts seem to support the idea that the small flux ropes are produced through magnetic reconnection across the heliospheric current sheet (Moldwin et al. 2000; Cartwright & Moldwin 2008, 2010). Using method similar to the one used by Cartwright & Moldwin (2010), we also investigated the time difference between the small-scale flux ropes listed in Feng et al. (2008) and the nearest sector crossing. Among the 81 flux ropes, we could only identify 35 events with clear sector crossing signature nearby, while Cartwright & Moldwin (2010) identified clear sector crossing signature in 71 cases out of the total 91 flux ropes. Cartwright & Moldwin (2010) presented the distribution of the time to the nearest sector crossing and found a sharp peak with 17 flux ropes

observed within 6 hr of a sector crossing. Among the 35 events we investigated, we found nine flux ropes observed within 6 hr of a sector crossing, but also found 18 flux ropes observed beyond one day of the nearest sector crossing. The fact that some flux ropes are very close to sector crossing and some others are far away from clear sector crossing, as demonstrated both in Cartwright & Moldwin (2010) and our investigation, suggests that a subset of the small-scale interplanetary flux ropes are likely to be produced through reconnection across the heliospheric current sheet. If the current sheet is locally tilted with respect to the passage of the spacecraft, the typical reconnection signature of one plasma jet within a current sheet should also be registered at the boundaries of newly formed flux ropes.

Some interplanetary small-scale flux ropes could also have a solar origin. This idea, proposed by Feng et al. (2007), Feng et al. (2008), and Wu et al. (2008), was supported by the continuous distribution of the duration of many small and intermediate-scale flux ropes, the similar solar cycle dependence of the occurrence rate between small flux ropes and magnetic clouds, and the similar energy spectrum between small flux ropes and solar flares. Wu et al. (2008) mentioned that due to the magnetic field inside small flux ropes being weaker than in magnetic clouds, particles can diffuse more easily and mix with each other between the flux ropes and the ambient medium, leading to little change in the proton temperature across a small flux rope. The magnetic pressure inside a small flux rope was proposed to be too small to drive expansion (Wu et al. 2008). Moreover, the increase in the size of small-scale flux ropes with increasing distance from the Sun recently discovered by Cartwright & Moldwin (2010) is similar to magnetic clouds and thus also supports the hypothesis of a similar origin of flux ropes with different scales.

In conclusion, we think that interplanetary small-scale flux ropes can be produced both in the solar wind and on the Sun. The reconnection signatures we identified at flux rope boundaries could either be related to the formation of flux ropes through reconnection across the heliospheric current sheet or result from subsequent interaction between flux ropes and the interplanetary magnetic fields after the initial formation of the ropes. Reconnection between magnetic clouds and interplanetary magnetic fields can peel off some magnetic field lines but may not efficiently reduce the size of magnetic clouds.

## 4. SUMMARY

We have performed the first systematic study of the boundaries of interplanetary small-scale magnetic flux ropes and identified signatures of magnetic reconnection at the boundaries. These signatures generally include a drop in the magnetic field magnitude and a plasma jet of $\sim$30 km s$^{-1}$ in a rotational field region. The reconnection regions often show additional properties such as a local increase of the proton temperature, density, and plasma beta.

We have examined the magnetic field and plasma parameters of 125 small-scale flux ropes reported in Feng et al. (2008) and found that 44 of them exhibit clear signatures of Alfvénic fluctuations. These flux ropes have been classified as Alfvén wave trains rather than as real flux ropes. We have found that about 42% of the flux ropes and 14% of the wave trains exhibit reconnection signatures at one or two boundaries. About 2/3 of the reconnection events at flux rope boundaries are associated with a shear angle larger than 90°, indicating fast anti-parallel reconnection. Among the reconnection exhausts found at flux rope boundaries, about 73% reveal a decrease by 20% or more in the magnetic field magnitude. More pronounced magnetic field depressions seem more likely to be associated with larger shear angles. These results suggest that reconnection at small-scale flux rope boundaries and in the background solar wind is distinctly different, with the former being much easier and faster.

We have also studied the occurrence rate of magnetic reconnection, average shear angle across reconnection exhausts, and average magnetic field depression inside reconnection regions at flux rope boundaries through the years 1995–2005 and found that all of these parameters seem to be relatively low/small around solar maximum and very high/large around solar minima.

The reconnection signatures we identified at small flux rope boundaries could either be related to the formation of flux ropes through reconnection across the heliospheric current sheet or result from the subsequent interaction between flux ropes and the interplanetary magnetic fields after the ropes are ejected from the Sun or formed in the solar wind. In the latter case, our study demonstrates that the boundaries of a substantial part of interplanetary small-scale flux ropes resemble those of magnetic clouds and thus imply a similar interaction process between flux ropes with different scales and the magnetic fields in the ambient medium.

We thank the data providers, R. Lepping at NASA/GSFC, R. Lin at UC Berkeley, and CDAWeb, for making the magnetic field and plasma data (obtained by *Wind*/MFI and *Wind*/3DP) publicly available. We also thank the anonymous referee for his/her effort in improving the paper. H.T. thanks Dr. H.-Q. Feng and A.-M. Tian for helpful discussions. The authors are supported by the National Natural Science Foundation of China under contracts 40874090, 40931055, and 40890162. The space physics group at PKU is also supported by the Beijing Education Project XK100010404, the Fundamental Research Funds for the Central Universities, and the National Basic Research Program of China under grant G2006CB806305.

## REFERENCES

Burlaga, L., Sittler, E., Mariani, F., & Schwenn, R. 1981, J. Geophys. Res., 86, 6673
Cane, H. V., & Richardson, I. G. 2003, J. Geophys. Res., 108, 1156
Cartwright, M. L., & Moldwin, M. B. 2008, J. Geophys. Res., 113, A09105
Cartwright, M. L., & Moldwin, M. B. 2010, J. Geophys. Res., doi:10.1029/2009JA014271
Cheng, X., Ding, M. D., Guo, Y., Zhang, J., Jing, J., & Wiegelmann, T. 2010, ApJ, 716, L68
Davis, M. S., Phan, T. D., Gosling, J. T., & Skoung, R. M. 2006, Geophys. Res. Lett., 33, L19102
Démoulin, P., & Dasso, S. 2009, A&A, 498, 551
Deng, X. H., et al. 2004, J. Geophys. Res., 109, A05206
Denskat, K. U., & Burlaga, L. F. 1977, J. Geophys. Res., 82, 2693
Eastwood, J. P., et al. 2005, Geophys. Res. Lett., 32, L11105
Feng, H. Q., & Wu, D. J. 2009, ApJ, 705, 1385
Feng, H. Q., Wu, D. J., & Chao, J. K. 2007, J. Geophys. Res., 112, A02102
Feng, H. Q., Wu, D. J., Lin, C. C., Chao, J. K., Lee, L. C., & Lyu, L. H. 2008, J. Geophys. Res., 113, A12105
Furno, I., et al. 2005, Phys. Plasmas, 12, 055702
Goldstein, H. 1983, in: NASA CP-228, On the Field Configuration in Magnetic Clouds, ed. M. Neugebauer (Washington, DC: NASA), 731
Gopalswamy, N., Lara, A., Yashiro, S., Nunes, S., & Howard, R. A. 2003, in Proc. ESA-SP 535, Solar Variability as an Input to the Earth's Environment, ed. A. Wilson (Noordwijk: ESA), 403
Gosling, J. T. 2007, ApJ, 671, L73
Gosling, J. T., Eriksson, S., & Schwenn, R. 2006a, J. Geophys. Res., 111, A10102
Gosling, J. T., McComas, D. J., Skoug, R. M., & Smith, C. W. 2006b, Geophys. Res. Lett., 33, L17102

Gosling, J. T., Phan, T. D., Lin, R. P., & Szabo, A. 2007a, Geophys. Res. Lett., 34, L15110
Gosling, J. T., Skoug, R. M., Haggerty, D. K., & McComas, D. J. 2005a, Geophys. Res. Lett., 32, L14113
Gosling, J. T., Skoug, R. M., McComas, D. J., & Smith, C. W. 2005b, J. Geophys. Res., 110, A01107
Gosling, J. T., Skoug, R. M., McComas, D. J., & Smith, C. W. 2005c, Geophys. Res. Lett., 32, L05105
Gosling, J. T., & Szabo, A. 2008, J. Geophys. Res., 113, A10103
Gosling, J. T., et al. 2007b, Geophys. Res. Lett., 34, L20108
Gosling, J. T., et al. 2007c, Geophys. Res. Lett., 34, L06102
He, J.-S., Marsch, E., Tu, C.-Y., Tian, H., & Guo, L.-J. 2010, A&A, 510, A40
He, J.-S., et al. 2008, J. Geophys. Res., 113, A05205
Innes, D. E., Genetelli, A., Attie, R., & Potts, H. E. 2009, A&A, 495, 319
Jian, L., Russell, C. T., Luhmann, J. G., & Skoug, R. M. 2006, Sol. Phys., 239, 393
Lee, L. C., Fu, Z. F., & Akasofu, S.-I. 1985, J. Geophys. Res., 90, 10896
Lepping, R. P., et al. 1995, Space Sci. Rev., 71, 207
Lepping, R. P., et al. 2006, Ann. Geophys., 24, 215
Lin, R. P., et al. 1995, Space Sci. Rev., 71, 125
Linton, M. G. 2006, J. Geophys. Res., 111, A12S09
Linton, M. G., & Moldwin, M. B. 2009, J. Geophys. Res., 114, A00B09
Liu, C. X., Jin, S. P., Wei, F. S., Lu, Q. M., & Yang, H. A. 2009, J. Geophys. Res., 114, A10208
Lundquist, S. 1950, Magnetohydrostatic Fields, Ark. Fys., 2, 361
Mandrini, C. H., Pohjolainen, S., & Dasso, S. 2005, A&A, 434, 725
Marsch, E., Yao, S., & Tu, C.-Y. 2009, Ann. Geophys., 27, 869
McComas, D. J., Gosling, J. T., Hammond, C. M., Moldwin, M. B., & Phillips, J. L. 1994, Geophys. Res. Lett., 21, 1751
Moldwin, M. B., Ford, S., Lepping, R., Slavin, J., & Szabo, A. 2000, Geophys. Res. Lett., 27, 57
Moldwin, M. B., Phillips, J. L., Gosling, J. T., Scime, E. E., McComas, D. J., Bame, S. J., Balogh, A., & Forsyth, R. J. 1995, J. Geophys. Res., 100, 19903
Okamoto, T. J., et al. 2007, Science, 318, 1577
Petschek, H. E. 1964, in NASA SP-50, The Physics of Solar Flares, ed. W. N. Hess (Washington, DC: National Aeronautics and Space Administration), 425
Phan, T. D., Gosling, J. T., & Davis, M. S. 2009, Geophys. Res. Lett., 36, L09108
Phan, T. D., et al. 2006, Nature, 439, 175
Pick, M., et al. 2005, ApJ, 625, 1019
Priest, E. R., & Forbes, T. G. 2000, Magnetic Reconnection: MHD Theory and Applications (Cambridge: Cambridge Univ. Press)
Richard, R. L., et al. 1989, J. Geophys. Res., 94, 2471
Ruan, P., et al. 2009, J. Geophys. Res., 114, 2108
Schwenn, R., & Marsch, E. 1991, Physics of the Inner Heliosphere, II. Particles, Waves and Turbulence (Berlin: Springer)
Shiota, D., Kusano, K., Miyoshi, T., & Shibata, K. 2010, ApJ, 718, 1035
Shitaba, K., & Uchida, Y. 1986, Sol. Phys., 103, 299
Shitaba, K., et al. 1994, ApJ, 431, L51
Slavin, J. A., et al. 2003, J. Geophys. Res., 108, A11015
Sonnerup, B. U. Ö., & Cahill, L. J., Jr. 1967, J. Geophys. Res., 72, 171
Tu, C.-Y., Marsch, E., Ivory, K., & Schwenn, R. 1997, Ann. Geophys., 15, 137
van der Holst, B., Jacobs, C., & Poedts, S. 2007, ApJ, 671, L77
Wang, Y. M., Wang, S., & Ye, P. Z. 2002, Sol. Phys., 211, 333
Wang, Y., Zheng, H., Wang, S., & Ye, P. 2005, A&A, 434, 309
Wei, F., Liu, R., Fan, Q., & Feng, X. 2003, J. Geophys. Res., 108, 1263
Wu, D. J., Feng, H. Q., & Chao, J. K. 2008, A&A, 480, L9
Xiao, C. J., et al. 2006, Nature Phys., 2, 478
Xiong, M., Zheng, H., & Wang, S. 2009, J. Geophys. Res., 114, A11101
Xiong, M., Zheng, H., Wu, S. T., Wang, Y., & Wang, S. 2007, J. Geophys. Res., 112, A11103
Yao, S., Marsch, E., Tu, C.-Y., & Schwenn, R. 2010, J. Geophys. Res., 115, A05103
Zong, Q. G., et al. 2004, Geophys. Res. Lett., 31, L18803